

Direct transfer of corrugated graphene sheets as stretchable electrodes

Junjun Ding, Frank T. Fisher, and Eui-Hyeok Yang

Citation: *Journal of Vacuum Science & Technology B* **34**, 051205 (2016); doi: 10.1116/1.4961594

View online: <http://dx.doi.org/10.1116/1.4961594>

View Table of Contents: <http://scitation.aip.org/content/avs/journal/jvstb/34/5?ver=pdfcov>

Published by the AVS: Science & Technology of Materials, Interfaces, and Processing

Articles you may be interested in

[Direct transfer and Raman characterization of twisted graphene bilayer](#)

Appl. Phys. Lett. **106**, 103107 (2015); 10.1063/1.4914309

[Ultraviolet/ozone treatment to reduce metal-graphene contact resistance](#)

Appl. Phys. Lett. **102**, 183110 (2013); 10.1063/1.4804643

[Graphene transparent electrodes grown by rapid chemical vapor deposition with ultrathin indium tin oxide contact layers for GaN light emitting diodes](#)

Appl. Phys. Lett. **102**, 162102 (2013); 10.1063/1.4802798

[Three-dimensional graphene foam-based transparent conductive electrodes in GaN-based blue light-emitting diodes](#)

Appl. Phys. Lett. **102**, 161902 (2013); 10.1063/1.4801763

[Noncatalytic chemical vapor deposition of graphene on high-temperature substrates for transparent electrodes](#)

Appl. Phys. Lett. **100**, 022102 (2012); 10.1063/1.3675632



AVS 63RD International Symposium & Exhibition
MUSIC CITY CENTER
Symposium: November 6-11, 2016 | Exhibit: November 8-10, 2016

www.avs.org

ERN MUSIC

Direct transfer of corrugated graphene sheets as stretchable electrodes

Junjun Ding, Frank T. Fisher, and Eui-Hyeok Yang^{a)}

Department of Mechanical Engineering, Stevens Institute of Technology, Castle Point of Hudson, Hoboken, New Jersey 07030

(Received 23 May 2016; accepted 12 August 2016; published 25 August 2016)

The authors present the fabrication and characterization of corrugated graphene sheets on polydimethylsiloxane (PDMS) substrates for flexible and stretchable electrodes. The graphene sheets were grown on imprinted Cu foil via atmospheric pressure chemical vapor deposition. The grown graphene sheets with both corrugated and flat surfaces were then transferred from the Cu foil to PDMS substrates using a novel, direct transfer method, where PDMS was directly casted and cured on the graphene sheets followed by removal of Cu via wet etching. This process largely eliminated the formation of cracks in the graphene caused by traditional transfer processes. The corrugated graphene sheets were characterized using Raman spectroscopy and conductivity measurements under the application of lateral strain parallel and perpendicular to the graphene corrugation on the PDMS substrates, demonstrating a smaller shift of the two dimensional Raman peak for the corrugated graphene electrodes as compared to the flat graphene. It was shown that the maximum achievable strain prior to a change in electrode resistance increased from 8% for the flat graphene sheet to 15% for the corrugated graphene electrode. Preliminary results also showed that the corrugated graphene sheet maintained its material integrity and electrical conductivity under multiple cycles of high strains. © 2016 American Vacuum Society.

[<http://dx.doi.org/10.1116/1.4961594>]

I. INTRODUCTION

Stretchable electrodes are a substantial component for flexible electronics such as flexible displays, flexible energy devices, smart skins, and wearable sensors.¹⁻⁶ Recent techniques are developed for transfer-printing inorganic devices onto flexible and stretchable substrates, including gecko-printing,⁷ microflaps,⁸ and spatula pads.⁹ Stretchable metal electrodes with high conductivity have been fabricated by formatting high aspect ratio metallic nanowire networks on a highly stretchable polymer substrate.^{10,11} Carbon nanomaterials such as carbon nanotubes, carbon fibers, and graphene have also been considered as alternative materials for flexible electrodes due to their high electrical conductivity, optical transparency, and mechanical flexibility.^{4,6,11-15} Graphene composite paper was made by coating a uniform layer of graphene oxide onto the surface of cellulose fibers. Then, a hydrothermal process was used to form porous reduced graphene oxide networks, which were not transparent.^{13,16} Chemical vapor deposition graphene films have been explored as a promising material for stretchable and transparent electrodes due to their atomic thickness and optical transparency.^{5,6,12,14,15,17-19} A buckled four-layer graphene electrode on a prestretched polydimethylsiloxane (PDMS) film was found to experience only a 0.2% variation in strain for tensile strains applied to the PDMS of up to 40%.¹⁷ Controlled crumpling and unfolding of large-area graphene sheets were also investigated, with results suggesting that the crumpled graphene-polymer laminates could be used as artificial-muscle actuators.¹⁸

For the application of graphene as stretchable electrodes, flexible substrates are typically prestretched before

transferring graphene onto the substrate. These preparation methods can be complicated, requiring a stretching stage to prestretch the substrates before the transfer of the graphene electrode. In addition, during the conventional graphene transfer process, a polymer layer such as poly(methyl methacrylate) (PMMA) is typically used as a support layer which is later removed. This polymer-removal step, typically involving a solvent such as acetone, will inevitably introduce small cracks in the graphene, which will result in a higher sheet resistance of the graphene electrode.²⁰⁻²²

Here, we report a new technique to transfer graphene onto polymer substrates by directly casting the polymer on graphene with a Cu foil substrate without using a support layer. For demonstration, PDMS is used as a target substrate to transfer graphene. By naturally casting PDMS, the cured PDMS maintains the same structure as the Cu foil while the copper is etched and the graphene is transferred to the PDMS substrates. Other polymers that can be coated on microstructured surfaces in the form of mixtures or dilute solutions and cured afterward could also be developed using a similar process. This transfer approach, in conjunction with the corrugated graphene sheet structure described below, shows promise as a means to increase electrode stretchability, while maintaining low sheet resistivity for stretchable electrode applications.

II. FABRICATION SCHEME

Figure 1 shows the fabrication sequence of the corrugated graphene electrode on PDMS. First, an acrylonitrile-butadiene-styrene (ABS) plastic grating mold with a period of 1 mm, spacing of 500 μm , and depth of 500 μm was prepared as a mold for a Cu foil. Subsequently, a 25 μm thick high purity Cu foil (5 \times 5 cm) (99.999% Alfa Aesar) was clamped

^{a)}Electronic mail: eyang@stevens.edu

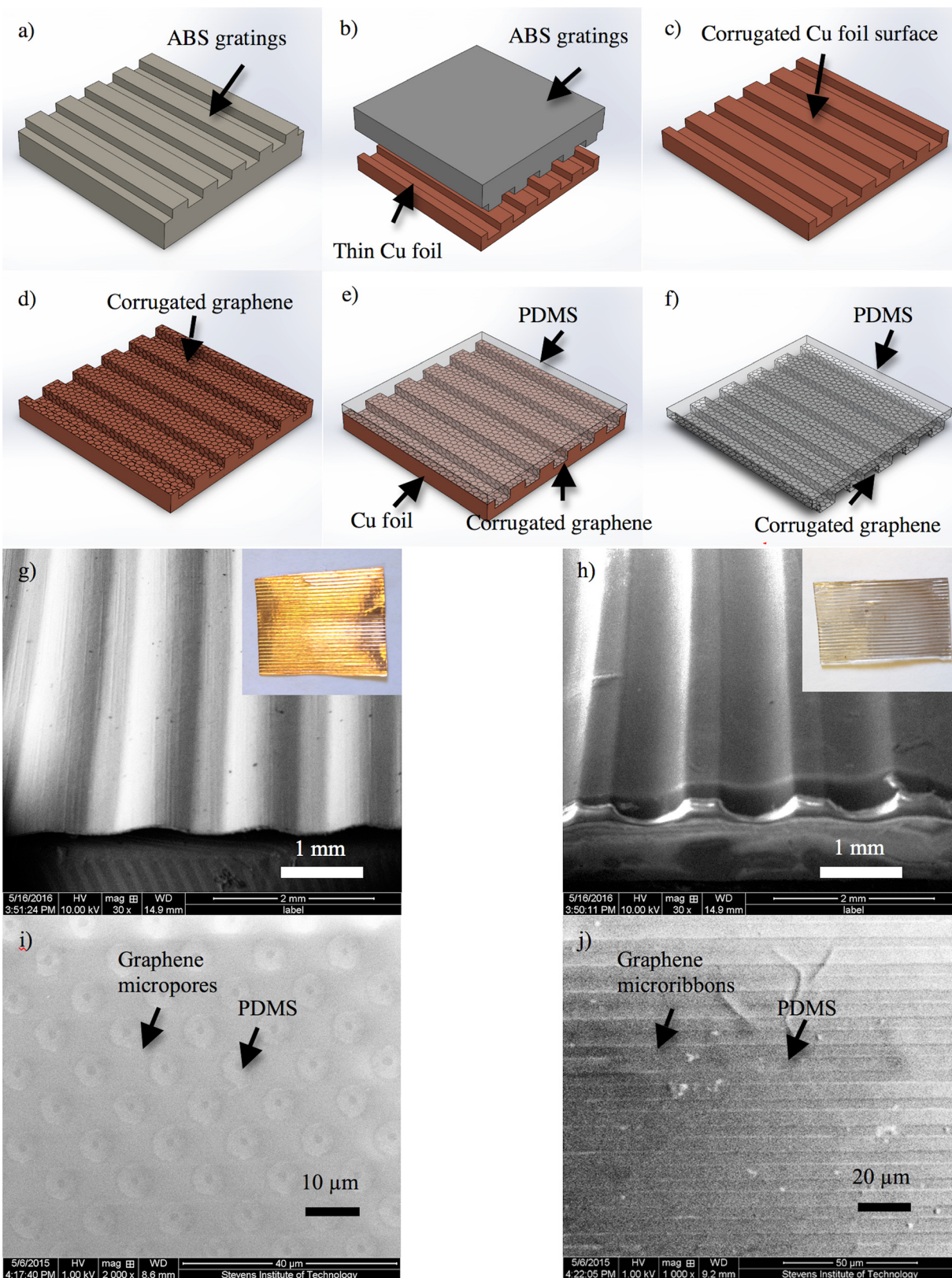


FIG. 1. (Color online) Schematic sequence for fabrication of a corrugated graphene electrode on a PDMS substrate. (a) ABS grating mold with period of 1 mm, spacing of 500 μm, and depth of 500 μm, (b) copper foil pressed by ABS grating mold, (c) corrugated copper foil, (d) graphene grown on copper, (e) liquid PDMS cured on graphene/copper, and (f) transferred graphene on PDMS after removal of the Cu foil. The figures are not drawn to actual scale. (g) Tilted SEM image of Cu foil with corrugated surface (insert image shows optical image of Cu foil with corrugated surface). (h) Tilted SEM image of corrugated graphene on PDMS (insert image shows optical image of corrugated graphene on PDMS). SEM images of (i) graphene micropore and (j) graphene microribbon patterns on PDMS surface, demonstrating that the transfer technique can be applied to various graphene patterns.

to the ABS plastic grating mold by a 6 in. bench mount mechanical vise, creating a corrugated Cu foil [Figs. 1(a)–1(c)]. The corrugated Cu foil was then placed in an atmospheric pressure chemical vapor deposition (APCVD) chamber, heated to 1000 °C at a rate of 30 °C/min with 1000 sccm Ar and 70 sccm H₂, and then annealed for 30 min at 1000 °C. Graphene growth was conducted for 40 s with 10 sccm CH₄. The chamber was cooled down at a rate of 60 °C/min to 400 °C and then to room temperature while keeping Ar and H₂ flowing at the same rates. It was observed using optical imaging²³ and Raman spectroscopy²⁴ that as a result of this process, two to four layers of graphene film were deposited on the surface of corrugated Cu foil [Fig. 1(d)]. In order to directly transfer the graphene to a flexible substrate while conserving the topology of the corrugated graphene shape, a liquid mixture of PDMS base and curing agent (Sylgard 184 Silicone Elastomer, Dow Corning) with a ratio of 10:1 by weight were thoroughly mixed and degassed under reduced pressure using a vacuum pump. The liquid mixture of PDMS was then casted on the surface of the corrugated graphene with Cu taped to the bottom of a plastic Petri dish. The sample was placed in a vacuum chamber to remove microbubbles in the PDMS, after which the PDMS was cured on a hot plate at 65 °C for 4 h [Fig. 1(e)]. PDMS at the backside of the graphene/Cu foil was removed by blade to expose the backside of the Cu foil. The copper foil was then etched for approximately 12 h in a citric acid etchant (Transene) bath and then placed in a fresh citric acid etchant for an additional 24 h to ensure the complete removal of copper, resulting in a corrugated graphene on PDMS sample [Fig. 1(f)]. A graphene on PDMS with a flat surface was fabricated using a regular Cu foil using the same fabrication sequence as described above and used as a control.

III. RESULTS AND DISCUSSION

Figures 1(g) and 1(h) show SEM and optical images (inset) of the pressed Cu foil with a corrugation period of 1 mm and height of 500 μm, and the corrugated graphene on PDMS substrate after PDMS transfer of graphene grown on the Cu foil. Compared to traditional transfer methods with PMMA as an interlayer,^{21,25} the PDMS direct transfer method maintains the integrity of the shape and structure of the corrugated graphene sheet with little damage. This is attributed to the lack of polymer supporting layer which is known to cause cracks in the graphene film by the build up of strain in the polymer layer during etching the Cu foil and transferring to target substrates.²⁰ Figures 1(i) and 1(j) show SEM images of separate graphene micropore and microribbon patterns on PDMS prepared by O₂ plasma etching of photolithography micropatterns of graphene on a copper substrate, demonstrating the broad applicability of the direct PDMS transfer method.

The graphene film grown on the corrugated Cu foil can be transferred to a PDMS substrate because of the van der Waals adhesion between the graphene film and the PDMS substrate.^{26,27} (In that work the flat graphene film could only withstand up to 1% strain before cracks were introduced in

the graphene film.) During the typical transfer process with PMMA as a support layer, there was inevitably stretching and folding in the PMMA film when transferring the graphene to target substrates. However, by our direct transfer method with PDMS, there was little stretch and bending applied to the graphene film to cause cracks; therefore, the electrically conductive sheet was preserved with a measured sheet resistance of 4.02 ± 0.50 kΩ/sq for the post-transferred graphene. This constant sheet resistance was observed for both the flat and corrugated graphene films.

It is important to note that there was no noticeable swelling observed during the etching process which is present would potentially cause microcracks in the graphene. PDMS swelling is a particular concern in nonpolar solvents such as hydrocarbons, toluene, and dichloromethane;²⁸ however, PDMS does not swell in contact with water.²⁸ The citric acid solution (Copper Etchant 49-1, Transene) used here to etch the Cu foils is a weak acid etchant. In addition, compared to the strain applied during the stretching test (up to 15% applied strain), the strain caused by swelling is negligible.

Due to the extremely low bending rigidity and significant flexibility of the graphene film, the corrugated graphene sheet on the PDMS substrate with a corrugated surface creates longer sheet length of the graphene film for high tensile strains prior to damage of the graphene.^{3,17} Figure 2 shows the peak shifts of the Raman spectra of the corrugated graphene on PDMS, characterizing the behavior of the samples subjected to tensile strain applied parallel or perpendicular to the graphene corrugation directions. Raman spectra were obtained using a 14 mW, 532 nm laser with a spot size of 3 μm to avoid excessive heating and damage to the sample surface. The Raman spectra for all samples were taken five times at different locations in the same sheet.

The D peak, G peak, and 2D peak positions in the Raman spectra were studied at various strains applied to the graphene on PDMS. The prominent peaks at ~1346, ~1590, and ~2686 cm⁻¹ are referred to as the D peak, G peak, and 2D peak of graphene, respectively. The D peak at ~1346 cm⁻¹ shows defects in the as-grown few-layer graphene film on the PDMS substrate. As shown in Fig. 2(a), when the tensile strain was applied parallel to the graphene corrugation ranges from 0% to 23.2%, the D peak varies from ~1343 to ~1347 cm⁻¹, and the G peak varies from ~1586 to ~1593 cm⁻¹. The D peak and G peak position trend lines shown in Figs. 3(a) and 3(b) indicate no major change in both the peak positions. The 2D peak position was used earlier as the key factor to investigate the strain in a flat graphene sheet up to 1% applied strain.^{29–31} As shown in Fig. 3(c), the 2D peak of the corrugated graphene on PDMS clearly red shifted from ~2686 to ~2671 cm⁻¹ under strain parallel to the graphene corrugation, indicating that the tensile strain leads to a morphology change in the graphene film causing strain in graphene. The corrugated surface does not increase the graphene length parallel to the graphene corrugation; therefore, the strain applied on the sample is imposed to the graphene sheet.

Figure 2(b) shows the Raman spectra of a corrugated graphene sheet on PDMS under tensile strain up to 15.99%

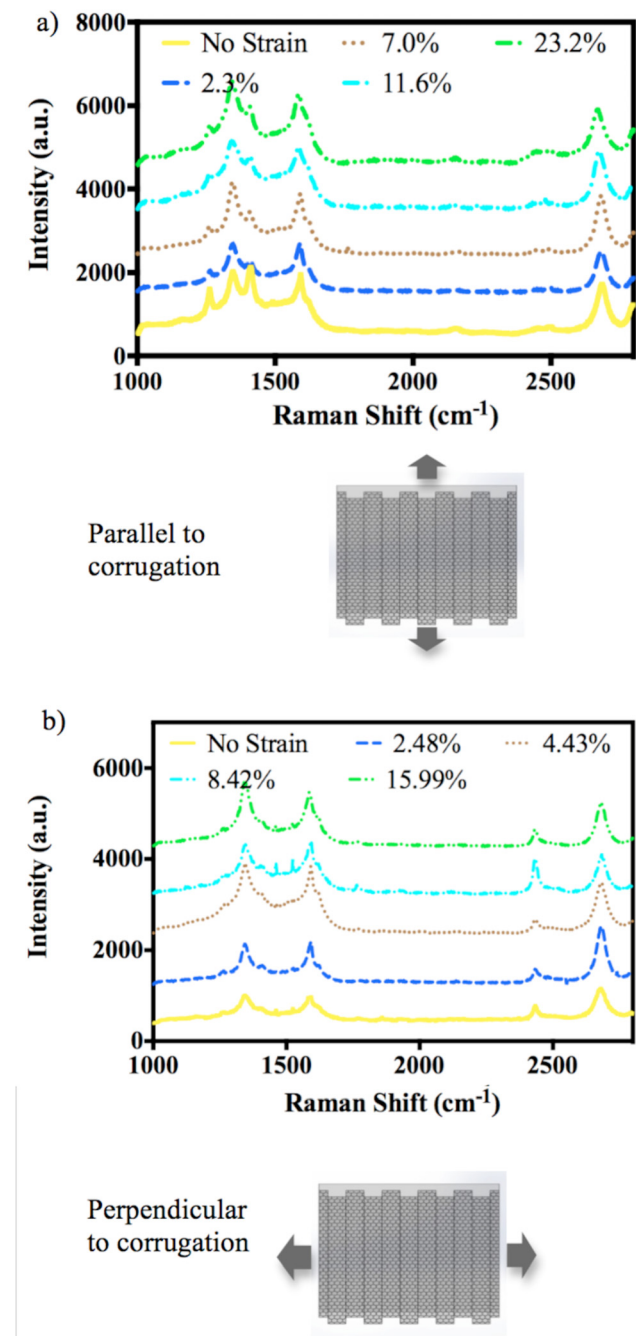


Fig. 2. (Color online) Raman spectra of corrugated graphene on PDMS under strain (a) parallel and (b) perpendicular to the graphene corrugation.

applied perpendicular to the graphene corrugation. The D peak varied from ~ 1344 to ~ 1347 cm^{-1} , while the G peak varied from ~ 1587 to ~ 1592 cm^{-1} . The D peak and G peak position trend lines shown in Fig. 3 indicate no major change in these peak positions. There was a minor shift of the 2D peak from ~ 2678 to ~ 2683 cm^{-1} , indicating that a small amount of strain was induced in the corrugated graphene film under strain perpendicular to the corrugation. These different shifts in the Raman peaks are attributed to the geometry of the corrugated graphene sheet on the PDMS substrate, where the corrugated graphene easily flexes along the direction perpendicular to the graphene corrugation, as compared to

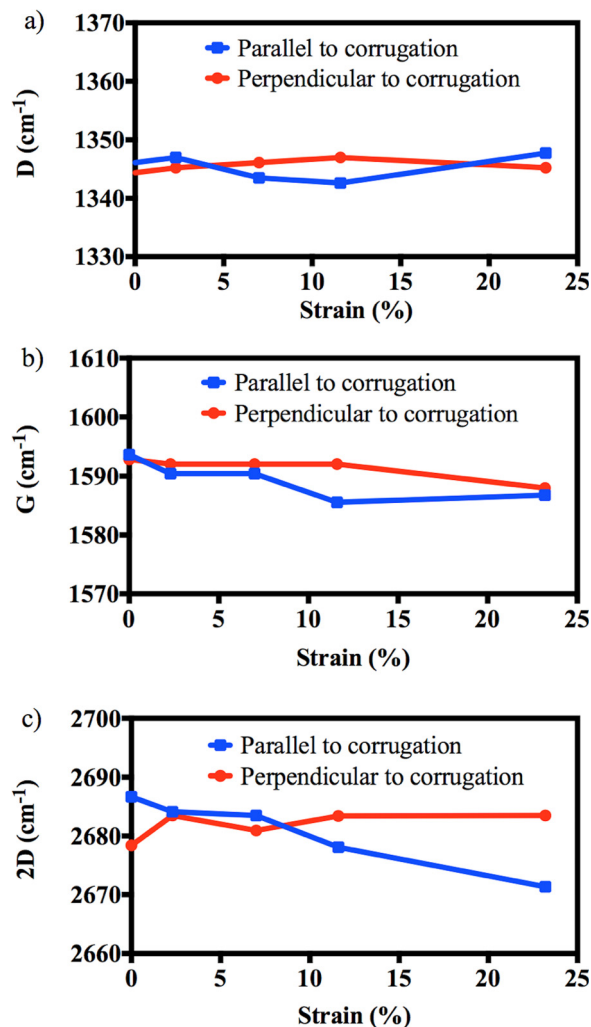


Fig. 3. (Color online) Shift of Raman (a) D, (b) G, and (c) 2D peaks of corrugated graphene under strain parallel and perpendicular to the graphene corrugation.

the graphene on a flat surface. Note that for flat graphene sheets, maximum strains on the order of 1% are generally reported in the literature.^{29,30}

The sheet resistance of graphene on PDMS was measured using a four-point probe method by passing current I through the outside two points of the probe and measuring the voltage V across the inside two points of the probe.³² Figure 4 shows a schematic of the four-point probe setup for the sheet resistance measurement, the sample stretching stage, and the sheet resistance measurement setup with the stretching stage. The four-point probe station is an S-302-4 manual four-point probe mounting stand with a Keithley 2000 multimeter and a Keithley 2200 power supply (Fig. 4). The four-point probe head (SP4-62045TBS, Lucas Signatone Corp.) is made of four tips with 0.254 mm radius and 1.587 mm spacing between adjacent tips. The graphene film is atomically thin and the edges of the graphene film are more than four times the spacing distance of the probe points. The graphene sheet resistance R_S can be determined based on the relationship³³

$$R_S = 4.53 \cdot V/I.$$

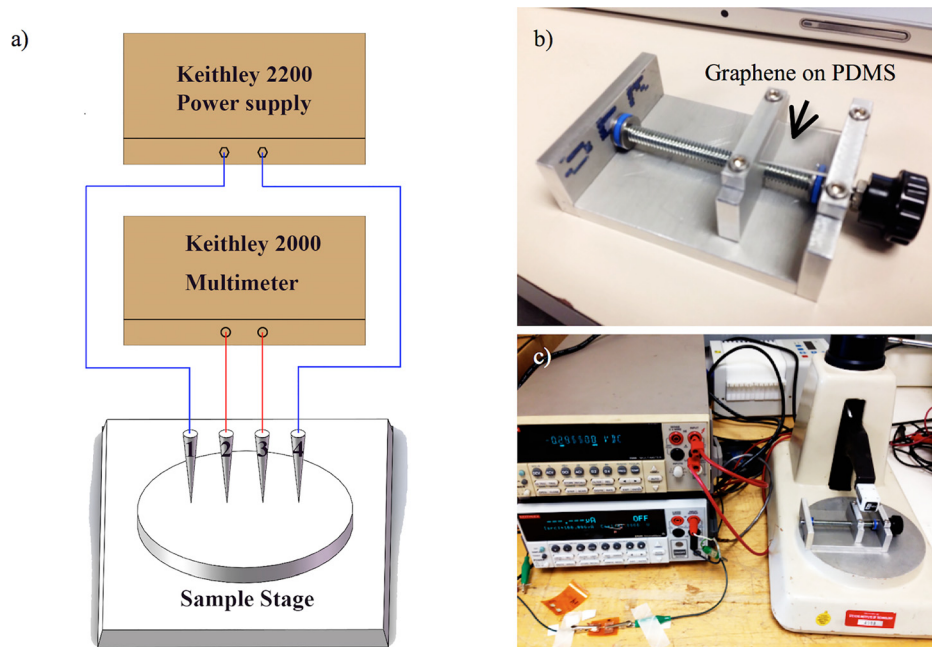


FIG. 4. (Color online) (a) Schematic of a four-point probe setup for graphene sheet resistance measurement. Photos of (b) stretching stage and (c) sheet resistance measurement setup with the stretching stage.

Figure 5 shows the measured sheet resistance of the corrugated graphene on PDMS with tensile strain applied parallel and perpendicular to the graphene corrugation, and the sheet resistance of graphene on a flat PDMS substrate under various tensile strains. Voltage between probes 2 and 3 was measured while applying current from 1 to 100 mA through probes 1 and 4. For all of the samples, initial sheet resistances of around 4.02 ± 0.50 k Ω /sq were measured based on the slope of a linear fitting of voltages versus current without any tensile strain applied. To apply the tensile strain on graphene on PDMS sample, the sample was clamped on both ends on the stretching stage shown in Fig. 4(b). The tensile strain applied on the sample was calculated by the lengths of the sample before and after stretching using a caliper.

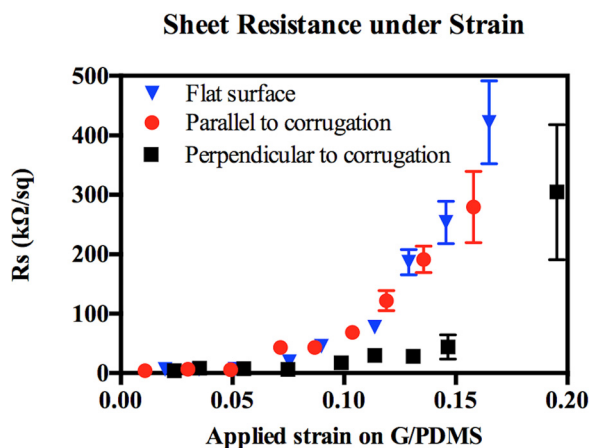


FIG. 5. (Color online) Sheet resistance of corrugated graphene on PDMS under the applied tensile strain parallel (red circles) and perpendicular (black squares) to the graphene corrugation. Flat graphene on PDMS under the same tensile strain is shown as a control (blue triangles). Each symbol represents the average of ten four-point probe measurements at various locations on the graphene surface.

When the tensile strain was applied parallel to the graphene corrugation, the sheet resistance of the corrugated graphene sheet on PDMS increased dramatically, closely following to the response of graphene on flat PDMS under tensile strain. This is due to the growth of cracks in the corrugated graphene film as the tensile strain that is applied parallel to the graphene corrugation increases, which is similar to graphene on flat PDMS because the corrugated surface does not increase the graphene “path” length parallel to the corrugation. Typically, a graphene sheet itself can only withstand no more than 1% of strain,^{29,30} before cracks form in the graphene sheet. This results in the rapid increase in the sheet resistance of the “flat surface” samples shown in Fig. 5. The sheet resistances at a tensile strain of 7% were around 44 k Ω /sq for flat and corrugated graphene on PDMS when the tensile strain was applied parallel to the graphene corrugation. Both sheet resistances increased dramatically beyond 8% tensile strain, which means the cracks in graphene film spread widely causing discontinuous graphene sheets.

However, when the tensile strain is applied perpendicular to the graphene corrugation, the sheet resistance of the corrugated graphene on PDMS under a 15% tensile strain was around 43 k Ω /sq, which is comparable to the sheet resistance of previous two samples at 8% tensile strain. The corrugated surface increased the graphene length by 100% due to the additional length of the vertical walls of the corrugated surface in comparison with the flat surface. It was shown that the maximum strain achievable prior to a change in resistance was increased from 8% for the flat graphene sheet to 15% for the corrugated graphene electrode. The corrugated graphene on PDMS was found to improve stretchability under the applied strain perpendicular to the graphene corrugation with little increase in its sheet resistance from the initial value.

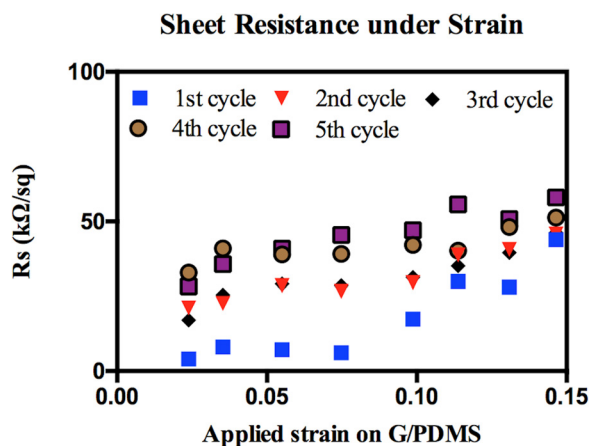


Fig. 6. (Color online) Sheet resistance of corrugated graphene on PDMS under tensile strain applied perpendicular to the graphene corrugation at multiple cycles. Each symbol represents the average of ten four-point probe measurements at various locations on the graphene surface.

The sheet resistance of corrugated graphene on PDMS was also measured as a function of multiple strain cycles applied perpendicular to the graphene corrugation with a maximum strain of 15% as shown in Fig. 6. The sheet resistance of the corrugated graphene on PDMS increased slightly after the first cycle of stretch, attributed to micro-cracks occurring in the graphene at the maximum strain. The cracks in graphene gradually grow under multiple cycles of stretch, while still keeping a relatively low sheet resistance ~ 55 k Ω /sq at the fifth cycle. These preliminary results indicate that at large tensile strains the corrugated graphene structure can still experience cracking, which is detrimental to the long-term electrical resistance of the corrugated graphene electrode and warrant further study.

There are several factors that contribute to graphene sheet conductance, including the graphene quality, cracks, or damage that form during the transfer step from as-grown substrate to the target substrate, and cracks produced by tensile strain in flexible substrates during daily usage.²⁴ The direct transfer of graphene by PDMS presented here is a simple and reliable way to transfer graphene from a Cu foil to a flexible substrate without using a polymer (usually PMMA) as a support material, whereas in the conventional transfer process, during PMMA removal process, cracks in graphene film are unavoidably produced.²⁰ In our method, minimal cracks and damage during the transfer process were observed as noted by the lack of change in the sheet resistance values. The transfer target could be replaced with any polymer that could be cured on graphene with the Cu substrate. In addition, the corrugated graphene on PDMS geometry was found to have enhanced stretchability perpendicular to the corrugation direction, resulting in a minimal increase in sheet resistance for small applied strains.

IV. CONCLUSIONS

We have introduced a simple and reliable graphene transfer method to a flexible substrate without using polymer such as PMMA as a support layer. The method simplifies the

transfer process and eliminates the polymer removal process, which was known to result in cracks in the graphene film. The transferred few-layer graphene on PDMS was measured with a sheet resistance of around 4.02 k Ω /sq. In order to increase the stretchability of graphene on PDMS, corrugated graphene on PDMS was fabricated by pressing of a thin Cu foil, followed by APCVD deposition of graphene, and PDMS direct transfer process. Examination of the 2D peak of the Raman spectra of the corrugated graphene on PDMS indicates minimal peak shifting for applied strains up to 16% (perpendicular to the graphene corrugation). Also, the sheet resistance measurements show that the corrugated graphene on PDMS exhibits sheet resistance values under 15% tensile strain perpendicular to the graphene corrugation comparable to resistance values found under 8% tensile strain parallel to the graphene corrugation. Lastly, cyclic strain results suggest that at large strains the corrugated graphene structure can still experience increases in electrical resistance, which may be attributed to damage that increases as the number of cycles increases. An examination of the impact of the maximum strain on the cyclic behavior of the corrugated graphene films and the optimization of the corrugation geometry will be topics of further study.

ACKNOWLEDGMENTS

This work has been partially carried out at the Micro Device Laboratory (MDL) funded with support from Contract No. W15QKN-05-D-0011. The authors would like to thank Eric Boon at Stevens Institute of Technology for sheet resistivity measurement.

- ¹D.-H. Kim, R. Ghaffari, N. Lu, and J. A. Rogers, *Annu. Rev. Biomed. Eng.* **14**, 113 (2012).
- ²T. Choi, S. J. Kim, S. Park, T. Y. Hwang, Y. Jeon, and B. H. Hong, *Nanoscale* **7**, 7138 (2015).
- ³H. H. Pérez Garza, E. W. Kievit, G. F. Schneider, and U. Staufer, *Nano Lett.* **14**, 4107 (2014).
- ⁴Y. Wang, L. Wang, T. Yang, X. Li, X. Zang, M. Zhu, K. Wang, D. Wu, and H. Zhu, *Adv. Funct. Mater.* **24**, 4666 (2014).
- ⁵Y. Xie, Y. Liu, Y. Zhao, Y. H. Tsang, S. P. Lau, H. Huang, and Y. Chai, *J. Mater. Chem. A* **2**, 9142 (2014).
- ⁶P. Xu, J. Kang, J.-B. Choi, J. Suhr, J. Yu, F. Li, J.-H. Byun, B.-S. Kim, and T.-W. Chou, *ACS Nano* **8**, 9437 (2014).
- ⁷J. Jeong, J. Kim, K. Song, K. Autumn, and J. Lee, *J. R. Soc. Interface* **11**, 99 (2014).
- ⁸B. Yoo, S. Cho, S. Seo, and J. Lee, *ACS Appl. Mater. Interfaces* **6**, 19247 (2014).
- ⁹S. Seo, J. Lee, K.-S. Kim, K. H. Ko, J. H. Lee, and J. Lee, *ACS Appl. Mater. Interfaces* **6**, 1345 (2014).
- ¹⁰P. Lee, J. Lee, H. Lee, J. Yeo, S. Hong, K. H. Nam, D. Lee, S. S. Lee, and S. H. Ko, *Adv. Mater.* **24**, 3326 (2012).
- ¹¹M.-S. Lee *et al.*, *Nano Lett.* **13**, 2814 (2013).
- ¹²T. Chen, Y. Xue, A. K. Roy, and L. Dai, *ACS Nano* **8**, 1039 (2014).
- ¹³L. Liu, Z. Niu, L. Zhang, W. Zhou, X. Chen, and S. Xie, *Adv. Mater.* **26**, 4855 (2014).
- ¹⁴R.-H. Kim *et al.*, *Nano Lett.* **11**, 3881 (2011).
- ¹⁵K. S. Kim *et al.*, *Nature* **457**, 706 (2009).
- ¹⁶H. Chen, M. B. Müller, K. J. Gilmore, G. G. Wallace, and D. Li, *Adv. Mater.* **20**, 3557 (2008).
- ¹⁷P. Xu *et al.*, *Carbon* **93**, 620 (2015).
- ¹⁸J. Zang, S. Ryu, N. Pugno, Q. Wang, Q. Tu, M. J. Buehler, and X. Zhao, *Nat. Mater.* **12**, 321 (2013).
- ¹⁹M. S. Brongseest, N. Bendiab, S. Mathur, A. Kimouche, H. T. Johnson, J. Coraux, and P. Pochet, *Nano Lett.* **15**, 5098 (2015).

- ²⁰C. Cai, F. Jia, A. Li, F. Huang, Z. Xu, L. Qiu, Y. Chen, G. Fei, and M. Wang, *Carbon* **98**, 457 (2016).
- ²¹J. Ding, K. Du, I. Wathuthanthri, C.-H. Choi, F. T. Fisher, and E.-H. Yang, *J. Vac. Sci. Technol., B* **32**, 6 (2014).
- ²²J. H. Hinnefeld, S. T. Gill, S. Zhu, W. J. Swanson, T. Li, and N. Mason, *Phys. Rev. Appl.* **3**, 014010 (2015).
- ²³H. Hidefumi, M. Hisao, and T. Kazuhito, *Appl. Phys. Express* **3**, 095101 (2010).
- ²⁴A. C. Ferrari *et al.*, *Phys. Rev. Lett.* **97**, 187401 (2006).
- ²⁵X. Li, Y. Zhu, W. Cai, M. Borysiak, B. Han, D. Chen, R. D. Piner, L. Colombo, and R. S. Ruoff, *Nano Lett.* **9**, 4359 (2009).
- ²⁶J. S. Bunch and M. L. Dunn, *Solid State Commun.* **152**, 1359 (2012).
- ²⁷K. Du, I. Wathuthanthri, Y. Liu, W. Xu, and C.-H. Choi, *ACS Appl. Mater. Interfaces* **4**, 5505 (2012).
- ²⁸J. N. Lee, C. Park, and G. M. Whitesides, *Anal. Chem.* **75**, 6544 (2003).
- ²⁹C. Neumann *et al.*, *Nat. Commun.* **6**, 8429 (2015).
- ³⁰X. Wang, K. Tantiwanichapan, J. W. Christopher, R. Paiella, and A. K. Swan, *Nano Lett.* **15**, 5969 (2015).
- ³¹T. Yu, Z. Ni, C. Du, Y. You, Y. Wang, and Z. Shen, *J. Phys. Chem. C* **112**, 12602 (2008).
- ³²M. B. Klarskov *et al.*, *Nanotechnology* **22**, 445702 (2011).
- ³³F. M. Smits, *Bell Syst. Technol. J.* **37**, 711 (1958).